RSC Advances

ROYAL SOCIETY OF CHEMISTRY

www.rsc.org/advances

An Environmental Friendly Process for the Synthesis of *f* GO Modified Anion Exchange Membrane for Electro-Membrane Applications

Prem P. Sharma[a,b], Swati Gahlot[a], Batuk M. Bhil[a], Hariom Gupta[a], Vaibhav Kulshrestha[a,b]*

[a]*CSIR-Central Salt and Marine Chemicals Research Institute (CSIR-CSMCRI), Council of Scientific & Industrial Research (CSIR),Gijubhai Badheka Marg, Bhavnagar- 364 002, (Gujarat), INDIA*
Fax: +91-0278-2566970.
E-mail: vaibhavk@csmcri.org, vaihavphy@gmail.com, Tel.: +91-2782567039. Fax: +91278-2567562.

[b] *Academy of Scientific and Innovative Research, CSIR-Central Salt and Marine Chemicals Research Institute (CSIR-CSMCRI), Council of Scientific & Industrial Research (CSIR), Gijubhai Badheka Marg, Bhavnagar- 364 002, (Gujarat), INDIA*

We report the synthesis of anion exchange membrane (AEM) based on chemically covalently modified graphene oxide (GO) for electrodialysis and fuel cell applications. GO was modified with silica (*f* GO) using APTEOS which involves epoxide ring opening reaction. The incorporation of silica particle within the GO flakes is characterized by TEM, EDX, XRD and FTIR while thermal stability is measured by TGA. Furthermore the successful development of membrane is done by incorporating *f* GO within quaternized polyethyleneimine (PEI) and poly(vinyl alcohol) by solution casting method followed by cross linking. The dispersiblity of silica modified graphene oxide is found to be very good within the polymer matrix. Membranes of various *f* GO content i.e. 1, 2, and 5 wt% within PEI matrix have been synthesized. Surface morphology and structural analysis of membranes are done using AFM, FTIR, XRD and ^{1}H NMR. Thermo mechanical analysis of membranes is done using TGA, DSC and UTM. Physicochemical and electrochemical analysis of the AEM are performed to quantify the ability for electro-membrane processes. *f* GO-PEI-2 membrane shows excellent electrochemical properties with comparable stability among the membranes. Furthermore the applicability of AEMs has been analyzed towards electrodialysis and fuel cell application. *f* GO-PEI-2 membrane show great potential for the electrodialysis and fuel cell application.

Key words: Polyethyleneimine; Functionalized Graphene oxide; Ionic conductivity; Thermo-mechanical properties.

Introduction:

Over the last decade research on the ion-exchange membrane (IEM) for either water or energy application is increasing tremendously [1-4]. IEM is a key component of both the technologies. For fuel cell IEM works as polymer electrolyte whereas for electrodialysis IEM is responsible for the movement of counter ions. Different types of ion exchange membranes are being used for fuel cell application [5,6]. Most fuel cell uses commercially available membrane Nafion which possesses excellent chemical and mechanical stability with higher ionic conductivity [7]. However, despite having such properties, the higher cost and low methanol cross over resistance and low applicability at high temperature impede the application in fuel cell. This giving the rise of need for production of efficient membranes for fuel cell application. Various kinds of IEMs have been developed by many researchers suitable for electrodialysis for water desalination [8-10]. Now days, more emphasis is being given to develop anion exchange membranes (AEM) owing to the advantages over cation exchange membranes such as use of non hazardous chemicals during synthesis and faster kinetics of oxygen reduction reactions etc. Whereas preparation of anion exchange membranes is being widely utilized for various, energy storage devices and electrochemical processes [11,12]. Polybenzimidazole (PBI) AEM with KOH doping is developed [13]. Quaternized polyethyleneimine (QPEI) based AEM with poly (vinyl alcohol) has also been prepared and tested for Direct methanol fuel cell (DMFC) [14, 15]. PVA possesses good film forming property, high hydrophilicity, easily available and it is also cost effective on the other hand quaternization of PEI provides mass nitrogen atoms of amine groups and thus there is abundance of anion exchange groups.

Graphene Oxide (GO) is a material of extensive research in the present days. The excellent mechanical and thermal stability combined with the high surface area make GO a distinct material [16]. The functional groups containing oxygen such as hydroxyl, epoxide, carbonyl and carboxyl groups in the structure of GO offers the possibility to bind with other materials and polymers [17, 18]. Poor dispersibility of GO hinders its use for many applications so it is essential to functionalize GO to prepare composites with enhanced dispersibility. The composites of GO possesses improved dispersibility as well as reinforces interfacial interactions required between graphene and the matrix. Nanocomposite of GO with silica has enhanced catalytic properties [19]. Now days, GO-composites are gaining much attention owing to their low cost

with superior physical and electrochemical properties. GO based composite membranes have been prepared and tested for different applications. Gahlot et. al. have developed GO/ SPES membranes for electrodialysis and fuel cell application [20]. Poly (ethylene oxide) and graphene oxide electrolyte membrane have been prepared and tested for low temperature polymer fuel cells [21]. Composite membranes based on SPEEK and SDBS-adsorbed graphene oxide have been synthesized and their performance evaluated for DMFC [22].

Generally the solvent used for AEM preparation is chloromethyl methyl ether (CME), which is very hazardous in nature and inhibited in India. To get rid of this hazardous chemical we tried a simple route to prepare AEM. In the present manuscript, *f* GO based nanocomposite anion exchange membranes of QPEI have been prepared and evaluated their performance by the means of salt removal and methanol permeability. Composite of GO with silica has been prepared and designated as *f* GO. Various *f* GO content (1%, 2% and 5%) is incorporated in Quaternized PEI (QPEI). Prepared membranes have been characterized for their structure and stability.

Experimental

Materials:

Polyethyleneimine with (average M_w~25000 g/mol), APTEOS (3-aminopropyltriethoxysilane), N,N-Dicyclohexylcarbodiimide (DCC-99%, M_w ~206.33 g/mol)and graphite powder are provided by Sigma Aldrich. PVA of (M_w~ 85000-1, 24,000 g/mol) is purchased from S D Fine CHEM LIMITED. Bromoethane (M_w ~ 108.97 g/mol) is procured by FINAR Chemicals. Other chemicals are purchased locally.

Synthesis of f-GO and Quaternized Polyethyleneimine:

Graphite powder is first converted into graphene oxide by oxidizing the natural graphite powder through modified Hummers method [6, 23]. Further graphene oxides having different functional groups such as hydroxyl, epoxide, carbonyl and carboxyl on its basal plane are reacted to APTEOS illustrated as follows. Briefly certain amount of graphene oxide as well as DCC (as catalyst) are dispersed in APTEOS followed by ultra-sonication for 1hr until homogeneous and brown colored mixture is obtained. Now this mixture was slowly stirred and kept for 24 hrs with

a continuous heating at 70^{o}C [24]. The reaction site is the epoxide ring that is present on the basal plane in graphene oxide. Now the resulting dark black colored homogeneous mixture of functionalized graphene oxide (*f* GO) is poured in ethanol further more centrifuged and washed with water several times and dried under vacuum. The schematic representation of the conversion of *f* GO from GO is shown in scheme 1. Firstly branched polyethyleneimine was dissolved in DMSO followed by the addition of certain amount of bromoethane and heated for 2-3 hours at 65 ^{o} C to get a transparent homogeneous quaternized polyethyleneimine (QPEI) solutiuon [25].

Synthesis of QPEI/f GO/PVA based nanocomposite membrane:

Poly (vinyl alcohol) was first dissolved in the dimethyl sulfoxide (DMSO) provided with a continuous stirring and heating (60 ^{o} C) until transparent and homogenous solution is obtained. To get a hybrid mixture of two different solutions, branched QPEI solution is added slowly. Now to enhance the mechanical and hydrothermal property APTEOS modified graphene oxide (*f* GO) was added drop wise in to it. The whole mixture was kept at 90^{o} C for 3 hrs with continuous stirring. The chemical reaction from the PEI to *f* GO-PVA-QPEI conversion is presented in scheme 2. After completion of reaction time the whole solution was slowly cooled at room temperature and casted on a glass plate and dried at 40^{o} C for 36 hours until the solvent is removed completely. To make it water insoluble it was then cross linked with formaldehyde solution.

Characterization of the membranes:

The materials and membranes are characterized by means of chemical, structural, mechanical and thermal techniques. Details are included in the Electronic Supplementary Information (ESI) section.

Physicochemical performance and Ionic conductivity of the membranes:

Water uptake, dimensional stability, Ion exchange capacity (IEC) and transport number of the membranes are measured using standard methods. Details are included in the Electronic Supplementary Information (ESI) section.

Ionic conductivity measurements of the composite membranes are conducted in different salt solution at 30 °C. Before measurements all the membranes are fully equilibrated with salt solution. For measurement the membranes are sandwiched between two circular stainless steel electrodes (1.0 cm^2). The membrane resistances are calculated from equation:

$$\sigma\ (\Omega^{-1}\ cm^{-1}) = \frac{L\ (cm)}{R\ (\Omega) \times A\ (cm^2)}$$

where L is the distance between the electrodes used to measure the potential, R is the resistance of the membrane, and A is the surface area of the membrane.

Methanol crossover resistance:

Resistance to methanol crossover of the membranes was evaluated by methanol permeability measurement in a cell. Membrane are placed between two compartments and 100 ml of methanol solution and 100 ml of deionised water is circulated in first and second compartment of the cell, respectively. The concentration of methanol in second compartment is measured as a function of diffusion time. The methanol permeability (P_M) was obtained by the equation [1];

$$P_M = \frac{1}{A} \frac{C_{II(t)}}{C_{I(t)} t} V_{II}\ l$$

where A is the effective membrane area, l the membrane thickness, $C_{II(t)}$ the methanol concentration in second compartment at time t, $C_{I(t)}$ the change in the methanol concentration in first compartment at time t, and V_{II} the volume of second compartment. For the suitability of membrane for fuel cell, we calculate the selectivity of the membrane by following equation;

$$S_P = \frac{\sigma}{P_M}$$

where P_M is the methanol permeability (cm^2/ s), and σ is the membrane conductivity ($S.cm^{-1}$).

Salt removal efficiency by electrodialysis:

PVC based ED cell with five compartments has been used to evaluate membrane performance for salt removal efficiency. The effective area of the membranes during ED was 66 cm^2 as shown in Fig. S-1. Constant DC potential is applied across the electrodes and the resulting current is

recorded using a power supply. 500 cm^3 of 0.1 mol dm^{-3} NaCl is circulated through compartment 1 (CC) while distilled water in compartment 2 (DC) at 4L/h in re-circulation mode. Adjacent to CC, 0.2 mol dm^{-3} Na_2SO_4 solution was fed into the electrode compartments to minimize the influence of electrode reactions. During ED process conductivity value is recorded at regular intervals to determine the ion concentration of DC and CC. Estimation of current efficiency and energy consumption has been done by the following equation [3, 8-10];

$$P\ (kWhkg^{-1}) = \frac{1}{m}\int UIdt$$

$$\eta = \frac{FnV\ (C_o - C_t)}{n_c \int Idt}\ X\ 100$$

where η is the current efficiency, F is Faraday constant, V is the volume of the dilute compartment (dm^{-3}), C_o and C_t are the concentration of dilute compartment at zero time and time t respectively, A is the membrane area, P is the power consumption, n is the stoichiometric number (n = 1 for NaCl), n_c is the number of cell pair, U is the applied voltage and I is current.

Results and Discussion

Structural Characterization:

As GO possess (-COOH) groups into its periphery, so the formation of amide bond take place by the reaction between (-OH) group of the carboxylic acid and hydrogen of amine present in PEI. In PVA and PEI, there is an electrostatic force of attraction in form of hydrogen bond between nitrogen present in PEI and hydrogen present in PVA. Chemical cross linking provide the stability to the membranes. Presence of different reactive groups on *f* GO (carboxyl, hydroxyl, epoxy etc.) and composite membranes are confirmed by FTIR and presented in Fig. 1. FTIR spectra of GO shows O-H stretching at 3402 cm^{-1}, C=O stretching at 1717 cm^{-1}, 1624 cm^{-1} and C-O stretching at 1051 cm^{-1}. In spectra of *f* GO the doublet at 3237 cm^{-1}, 2925 cm^{-1} attributes to the symmetric Vs CH and asymmetric Vs CH_2 of the alkyl chains of silane moieties. Peak at 1584 cm^{-1} in *f* GO corresponds to C-C stretch in aromatic ring and at 1025 cm^{-1} is due to the

presence of Si-O-C and Si-O-Si bond. FTIR of composite membranes displays the grafted functional groups onto the membranes. QPEI membrane shows stretching peak at 3615 cm^{-1} while *f* GO-PEI-5 at 3642 cm^{-1} is due to O-H vibrations. Presence of peaks at 2347 cm^{-1} and 2350 cm^{-1} in QPEI and *f* GO-PEI-5 respectively is due to the stretching vibration. Peak at 1189 cm^{-1} and 1176 cm^{-1} in QPEI and *f* GO-PEI-5 respectively is corresponds to C-N stretching. Peaks between 650 cm^{-1} - 1000 cm^{-1} attributes to the =C-H stretching. Peak values at 1693 cm^{-1} in QPEI and 1710 cm^{-1} in *f* GO-PEI-5 are attributed to the α, β unsaturated carbonyl groups. There is a shift in peak towards higher value in *f* GO-PEI-5 which is due to the interaction between *f* GO and QPEI matrix.

The FT-NMR spectra of QPEI, *f* GO and *f* GO-PEI-5 are presented in Fig. 2 (A, B & C). In Fig. 2 (A) ^{1}H NMR analysis of quaternised polyethylenimine shows a chemical shift value due to mainly three different type of protons. The chemical shift value nearby to 1.6 ppm to 2.46 ppm is due to the interaction between the protons connected to the –C=C– (ethylene group) and amine group. The multiplet peak near to this reason shows the merging of splitted signals due to the interaction of more than one type of protons that are in different environment corresponding to each other. While triplet signal nearby to 3.00-3.26 ppm indicates the protons interaction between (–C=C-) ethylene group. The singlet peak nearly to 4.00 ppm indicates about the presence of same kind of protonic with respect to surrounding environment. In Fig. 2 (B) singlet peak at 1.3 ppm indicates the presence of protons corresponding to –C=C– group present in the benzene ring. Several peaks at chemical shift values 2.2-3 ppm shows the presence of benzylic Ar-C-H. The peaks in the area of chemical shift 3.4-4.0 ppm values shows the interaction of protons attached to ethylene group with that of proton attached to more electronegative oxygen atom in –OH (hydroxyl group) group.

Fig. 3 shows the XRD patterns for GO, *f* GO and *f* GO-PEI-5. It can be seen from XRD curve GO represents the sharp peak at 11.4° agreeing well with previous literature [26]. After modification of GO with silica XRD peak is shifted to 11.1° corresponds to GO while a new peak is observed at 21.8° is due to the interaction of silica with GO [27]. The inter-planar spacing in GO and *f* GO are found to be at 8.1 Å and 7.9Å respectively, the reduction in interplanar spacing is due to decoration of silica nanoparticles on GO. *f* GO-PEI-5 composite membrane shows the diffraction peaks at 9.68° and 19.11° which is due to the interaction

between *f* GO and QPEI matrix. The structure of GO are presented in Fig. 4(B, C) as the TEM images. It is self explanatory that the structure of GO is found to be layered. The flakes of *f* GO can be seen in SEM as Fig. 4(A). The TEM images of silica modified GO (*f* GO) at different magnification can be seen in Fig. 4 (D, E & F). Figure shows the uniformly distributed Si nanoparticles on to the GO flakes surface. The elemental mapping of *f* GO is also performed to confirm the distribution of silica in *f* GO. Fig. 5 shows the elemental mapping of C, O and silica in different colours and confirms the uniform distribution on silica. The change in transparency of the membranes is presented in Fig. 6 as the photographs. It is clear from the figure that all the membranes are transparent in nature but the transparency decreases by increasing the *f* GO in to the membrane matrix. AFM images of *f* GO-PEI-1 (Fig. 7 (A, A')) and *f* GO-PEI-5 (Fig. 7 (B, B')) represent the 2d and 3d view of membranes. It is clear from the figures that roughnesses of the membranes increases with the *f* GO content in PEI matrix, which can be enhance the transport due to higher surface area.

Thermo-mechanical Analysis of hybrid Anion exchange membranes:

DSC of quaternized PEI and other *f* GO composite membranes are shown in Fig. S-2. Glass transition (T_g) of QPEI membrane is observed at about 110°C which goes to increase by the incorporation *f* GO and reaches to 120°C for *f* GO-PEI-5 membrane. Fig. S-3 and S-4 displays the TGA and DTG thermogram of all membranes. Three step weight losses occur in membranes, first weight loss between 100-150°C is due to the loss of bound water and absorbed water onto membrane. Second stage weight loss has been observed around 250-400°C due to decomposition of bromomethyl groups in PEI. Last weight loss between 450-500°C is attributed to decomposition of polymer backbone. There has not been observed a significant change in the decomposition temperatures of *f* GO-PEI composite membranes with *f* GO concentration. Strain-stress curves of the membranes are presented in Fig. 8 and the corresponding values for elastic modulus, stress and maximum elongation are shown in Table 1. It is found from the table that ~~on~~ increasing *f* GO content effects the mechanical properties of the membranes. The stress value of the composite membranes (*f* GO-PEI-2) is found to be twice to the QPEI membrane as shown in table 1. Increased value of stress is because of the better interaction between QPEI and *f* GO and also due to excellent mechanical strength of GO. The elastic modulus and strain decreases with

increasing *f* GO it may due to increment of rigid and brittleness of the membranes but the values of elastic modulus and strain sufficiently enough to use these membranes to any electro-membrane processes application.

Physicochemical and Electrochemical Characterization of the hybrid Anion Exchange Membranes:

Water retention capability, water uptake behaviour, ion exchange capacity and transport number of different membranes are presented in Table 2. Water uptake and retention play an important role in IEMs for migration of ions during electro-membrane processes. Water uptake of the QPEI membrane is calculated to 40%, which goes to increases by increasing *f* GO content in to the QPEI matrix. The water uptake reaches to 61% for *f* GO-PEI-5 membrane, the value is 50% higher that of QPEI, due to the more hydrophilic nature of *f* GO. Two types of water available in IEMs: bound water and the free water. Bound water found to be more responsible for the ion conduction. The amount of bound water is calculated by TGA analysis from 100-150 °C [6], while the free water is the difference of total water to the bound water. QPEI membranes shows the lowest bound water content (0.6 %) in comparison with all membranes while 1.3% bound water in *f* GO-PEI-5 composite membrane, more bound water in *f* GO-PEI-5 make it higher water retention availability and higher ionic conducting. Unfortunately the higher water uptake reduces the mechanical stability but no reduction has been recorded in this case due to interaction of *f* GO with QPEI matrix [1, 20]. IEC values increases with the increment in the concentration of *f* GO in QPEI and reaches to 3.31 meq/g for *f* GO-PEI-2, which is 23% higher to QPEI due to presence of more functional group in matrix. Counter ion transport number of the membranes is measured by Hittorf method using different concentration of salt solution in a diffusion cell. The transport number of QPEI is 0.81 which is lower than *f* GO-PEI-2 membrane, and comparable to the commercial IEMs [10].

Ionic conductivity of different membranes depend upon the different parameters like presence of functional group, IEC, water uptake, bound water content etc., and are presented in Table 3. The value of ionic conductivity is found be increasing with increased amount of *f* GO within QPEI matrix. *f* GO-PEI-2 demonstrates the maximum ionic conductivity 7.8 x 10^{-2}S/cm which is 56%

higher than QPEI and 8% higher than *f* GO-PEI-5. This increase in value is due to the increased number of functional *f* GO and higher ion transport through *f* GO-PEI-2. The value of ionic conductivity increases with increasing salt concentration as presented in Fig. 9. The dependence of ionic diffusion coefficient on *f* GO content is evaluated by the Nernst-Einstein equation using membrane conductivity [28]. Diffusion coefficient of the membranes is also found to be increasing by incorporation of *f* GO and presented in Table 3. The results indicate that *f* GO increasing the applicability of the membrane for different electro-membrane processes.

Methanol permeation (P_M) resistance and selectivity of hybrid Anion exchange membranes::

High ionic conductivity and low methanol permeation are the essential requirement of membrane for fuel cell application. Table 3 shows the methanol permeability of QPEI and *f* GO/QPEI membranes. It is clear from the data that methanol permeability of *f* GO/QPEI membranes decrease with increment of *f* GO content. Since *f* GO acts as a barrier and obstruct the movement of methanol within the interconnected hydrophilic channels owing to the interaction between *f* GO and QPEI. The interaction between *f* GO and QPEI restricts the formation of the channels in membranes, which leads to higher methanol permeation resistance. Methanol permeability for the QPEI membrane is calculated to 4.827 X 10^{-7} cm^2S^{-1}, which reduces to 4.156 X 10^{-7} cm^2S^{-1} for *f* GO-PEI-1, 4.035 X 10^{-7} cm^2S^{-1} for *f* GO-PEI-5 and reaches to 3.958 X 10^{-7} cm^2S^{-1} for *f* GO-PEI-2 membranes. The strong interfacial adherence of *f* GO particle with the QPEI matrix makes the membrane less permeable for methanol [29]. To make a membrane more selectively suitable for fuel cell application it should be directly proportional with respect to membrane conductivity and should be inversely proportional to methanol permeability. This selectivity can be seen in Table 3 that found to be 5.66X10^4 for QPEI and raises to 8.14X10^4 for *f* GO/QPEI-2 as we increase the *f* GO content in membrane matrix. The tendency of the membrane for highly resistive toward methanol and higher selectivity make them more suitable for fuel cell application.

Electrodialytic performance of hybrid Anion exchange membranes:

Fig. 10 shows the current-voltage *(i-v)* characteristics of different composite membranes equilibrated on 0.1 M NaCl solution. Three typical characteristic regions, viz., Ohmic, plateau

and non-Ohmic can be seen from *i-v* curves which reveal the concentration polarization and ion transport phenomenon across the anion exchange membranes [30, 31]. In the first region current increases with applied potential, in second region current remains constant and in third region or over-limiting region ions get depleted in solution causing water splitting and get high current density on increasing potential (Fig. 10).

Salt removal efficiency from water, of the developed membranes are observed during Electro-dialysis (ED) experiments. ED is performed at constant applied potential (2.0 V/Cell pair) using 0.1 mol dm^{-3} NaCl solution as feed for diluted compartment (DC), while deionized water is circulated in concentrated compartment (CC) and Na_2SO_4 solution (0.02 mol dm^{-3}) through both electrode rinse compartments, in the recirculation mode. The suitability of developed membranes for desalination applications are assessed in terms of estimating current efficiency and energy consumption for salt removal. Variation in salt concentration in DC with time during electrodialysis is shown in figure Fig. 11(A). Initially concentrations of DC depleted with time in the linear fashion and goes to slower after 180 min., this mey be due to the depletion of ion in DC compartment. The concentration of DC depleted faster with *f* GO-PEI-2 membrane than other due to its higher transport number and ionic conductivity that make easy the transport of ions. The concentration of DC decreases from 0.1 – 0.01 mol dm^{-3} in 265 minute with *f* GO-PEI-2 membrane while it takes 322 minute time with QPEI membrane for same concentration (Fig. 11(A)), while 300 min. and 278 min. time is taken by *f* GO-PEI-1 and *f* GO-PEI-5 membrane respectively for the same amount of salt removal. Fig. 11 (B) shows the change in the conductivity of DC and CC with time during salt removal, as conductivity of DC decreases its increases for CC. The decrement in conductivity of DC with *f* GO-PEI-2 membrane is faster than QPEI due to its higher diffusion coefficient and ion migration. There is no change in pH during salt removal. The *f* GO-PEI-2 membrane shows superior electro-transport properties among the membranes and can be used for the water desalination.

Power consumption and current efficiency data to evaluate the performance of composite membranes are presented in Table 4. During the salt removal the power consumption decreased, while current efficiency increased with *f* GO content in QPEI matrix. Power consumption and current efficiency depend on operating conditions of experiment and electrochemical properties of membranes. The CE and *P* for the *f* GO-PEI-2 membrane are found to be 93% and 0.86 kWh

kg^{-1} respectively, while 83.5% and 1.097 kWh $kg^{-1}$for QPEI membrane which shows the potential of the composite membrane for electro-membrane processes.

Conclusion:

Graphene oxide (GO) nano sheet have been successfully synthesised by modified Hummer's methods and further modified by APTEOS. The uniform distribution of silica in GO is confirmed by elemental mapping. The composite of QPEI with different content of *f* GO, shows the higher thermal and mechanical stability. The ionic conductivity of the AEM increases with *f* GO content in PEI for all the membranes. The high ionic conductivity of composite membrane is due to the intermolecular interactions between *f* GO and QPEI, and also presence of different functionality on *f* GO, which remarkably increased ionic diffusion. In summary the influence of *f* GO on different membrane properties is relevant for electro-membrane processes. *f* GO-PEI-2 membrane shows the highest ionic conductivity and selectivity that is 7.2 x 10^{-2} Scm^{-1} and 7.15 x 10^4 cm^2 S^{-1} respectively. The value for ionic conductivity is 50% higher and selectivity is 33% higher than that of QPEI which has 5.0 x 10^{-2} Scm^{-1} and 5.66 x 10^4 cm^2 S^{-1} respectively. The power consumption and current efficiency values during salt removal using *f* GO-PEI-2 membrane are calculated to be 0.98 $kWhkg^{-1}$ and 94.01% respectively. Power consumption is 20% lower and 12 % higher current efficiency is achieved compared to QPEI membrane. According to the results the membrane is highly stable and shows the higher ionic transport efficiency as well the process for synthesis of the membrane is environmental friendly. Incorporation of *f* GO in QPEI is confirmed to be excellent scheme to enhance the electrochemical and physicochemical properties of SPES membranes.

Acknowledgments

Author V. Kulshrestha is thankful to Department of Science and Technology, New Delhi, for providing fund under WTI scheme. Financial support received from CSIR Network projects (CSC 0105 and CSC 0115) is also acknowledged. Authors are also thankful to Analytical Discipline and Centralized Instrument facility, CSMCRI, Bhavnagar for instrumental support.

Supporting Information:

The detail of the chemical, structural, physiochemical characterization & membranes stability are included as section S1-S3 in supporting information. Fig. S-1 to S-4 are also included in supporting information section.

References:

1. Gahlot, S.; Kulshrestha, V. *ACS Appl. Mater. Interfaces*, **2015**, *7*, 264.
2. Tanaka, Y. *Desalination*, **2012**, *301*, 10.
3. Gahlot, S.; Sharma, P.P; Kulshrestha, V. *Separation Science and Technology,* ***2015,*** 50, 446.
4. Perumal, B.; Dharmalingam S. *Energy,* **2011**, *36,* 3360.
5. Fen, K.; Tang, B.; Wu, P *J. Mater. Chem*. **2014**, *2,* 16083.
6. Gahlot, S.; Sharma, P.P; Kulshrestha, V.; Jha, P. K. . *ACS Appl. Mater. Interfaces* **2014**, *6,* 5595.
7. Sahu, A. K.; Pitchumani, S.; Sridhar, P.; Shukla, A. K. Bull. *Mater. Sci*. **2009,** *32,* 285.
8. Chatterjee, U.; Jewrajka, S. K. *J. Mater. Chem. A*, **2014,***2,* 8396.
9. Chatterjee, U.; Bhadja, V.; Jewrajka, S.K. *J. Mater. Chem. A*, **2014**, *2,* 16124.
10. Sharma, S.; Dinda, M.; Sharma, C. R.; Ghosh, P. K. *J Membrane Science*, **2014**, *459*, 122.
11. Wang, J.; Qiao, J.; Baker, R.; Zhang. J. *Chem. Soc. Rev*., **2013**, *42,* 5768.
12. Jheng, Li-C.; Hsu, S. L.; Tsaia T. Y.; Chang, W. J.Y.; J. Mater. Chem. A, **2014**, 2, 4225
13. Li, N.; Wang, L.; Hickner, M.; *Chem. Commun.,* **2014**, 50, 4092
14. Xu, P. Y.; Guo, T. Y.; Zhao, C. H.; Broadwell, I.; Zhang, Q. G.; Liu, Q. L. *J. Appl. Polym. Sci.*, **2013**, *128*, 3853.
15. Sheng, L.; Higashihara, T.; Nakazawab, S,; Ueda, M.; Polym. Chem., **2012**, 3, 3289
16. Zhu , Y.; Murali , S.; Cai , W.; Li , X.; Suk , J. W.; Potts, J. R.; Ruoff, R. S. *Adv. Mater.* **2010**, *22,* 3906.
17. Novoselov, K. S.; Geim, A. K.; Morozov, S. V.; Jiang, D.; Zhang, Y.; Dubonos, S. V.; Grigorieva, I. V.; Firsov, A. A. *Science* **2004**, *306*, 666.
18. Zhao, G.; Wen, T.; Chen, C.; Wang, X. *RSC Advances*, **2012**, *2,* 9286.
19. Zhang, W. L.; Choi, H. J. *Langmuir*, **2012,** *28,* 7055.

20. Gahlot, S.; Sharma, P.P; Gupta, H.; Kulshrestha, V.; Jha, P. K. *RSC Adv.*, **2014, *4,*** 24662
21. Cao, Y. C.; Xu, C.; Wu, X.; Wang, X.; Xing, L.; Scott, K. A *Journal of Power Sources,* **2011**, *196,* 8377.
22. Jiang, Z.; Zhao, X.; Fu, Y.; Manthiram, A. *J. Mater. Chem.* **2012**, *22*, 24862.
23. Chen, D.; Feng, H.; Li, J. *Chem. Rev.* **2012**, *112*, 6027.
24. Yang, H.; Li, F.; Shan, C.; Han, D.; Zhang, Q.; Niu, L.; Ivaska, A. *J. Mater. Chem*. **2009**, *19,* 4632.
25. Xu, P. Y.; Guo, T. Y.; Zhao, C. H.; Broadwell, I.; Zhang, Q. G.; Liu, Q. L. *J.Appl. Polym. Sci.,* **2013,** *128* ,3853.
26. Zhang, W. L.; Park, B. J.; Choi, H. J. *Chem. Commun.* **2010**, *46,* 5596.
27. Zeng, C.; Tang, Z.; Guo, B.; Zhang, L. *Phys. Chem. Chem. Phys*., **2012**, *14,* 9838.
28. Hoarfrost, M.L.; Tyagi, M.S.; Segalman, R.A.; Reimer, J.A. *Macromolecules* **2012**, *45*, 3112.
29. Tseng, C.Y.; Ye, Y.S.; Cheng, M.Y.; Kao, K.Y.; Shen, W.C.; Rick, J.; Chen, J.C.; Hwang, B.J. *Adv. Energy Mater.* **2011**, *1*, 1220.
30. Chakrabarty, T.; Rajesh, A. M.; Jasti, A.; Thakur, A. K.; Singh, A. K.; Prakash, S.; Kulshrestha, V.; Shahi, V. K. *Desalination* **2011**, *282*, 2.
31. Strathmann, H.; Electrodialysis. In *Membrane Separations Technologys Principles and Applications*; Noble, R. D., Stern, S. A., Eds.; Elsevier Press: Ireland, **1995**.

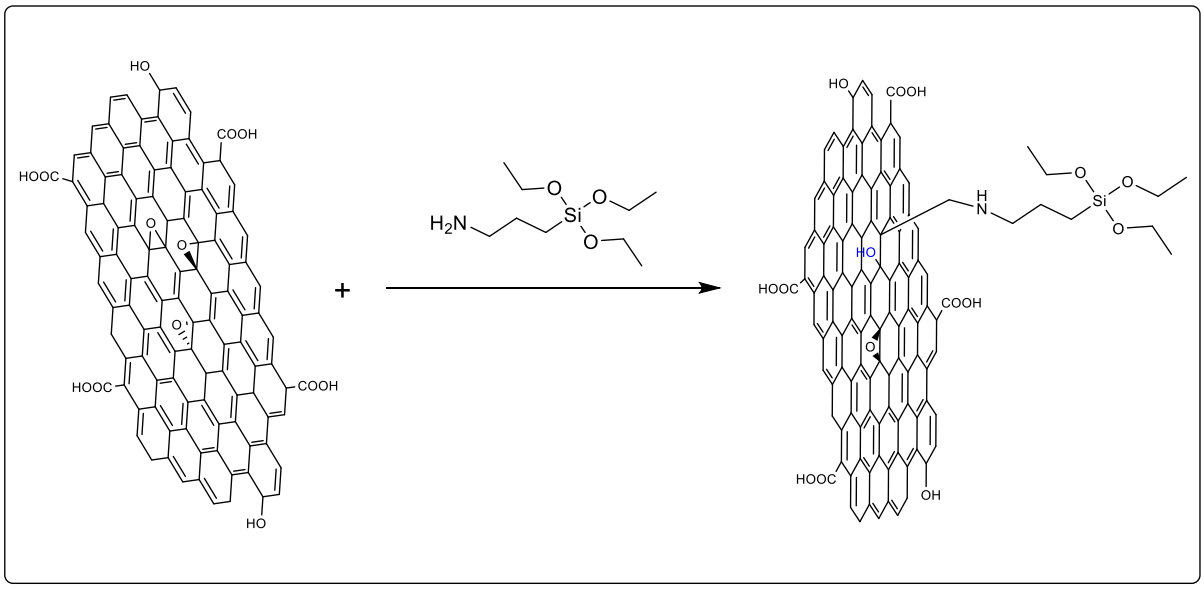

Scheme 1: Functionalization of GO

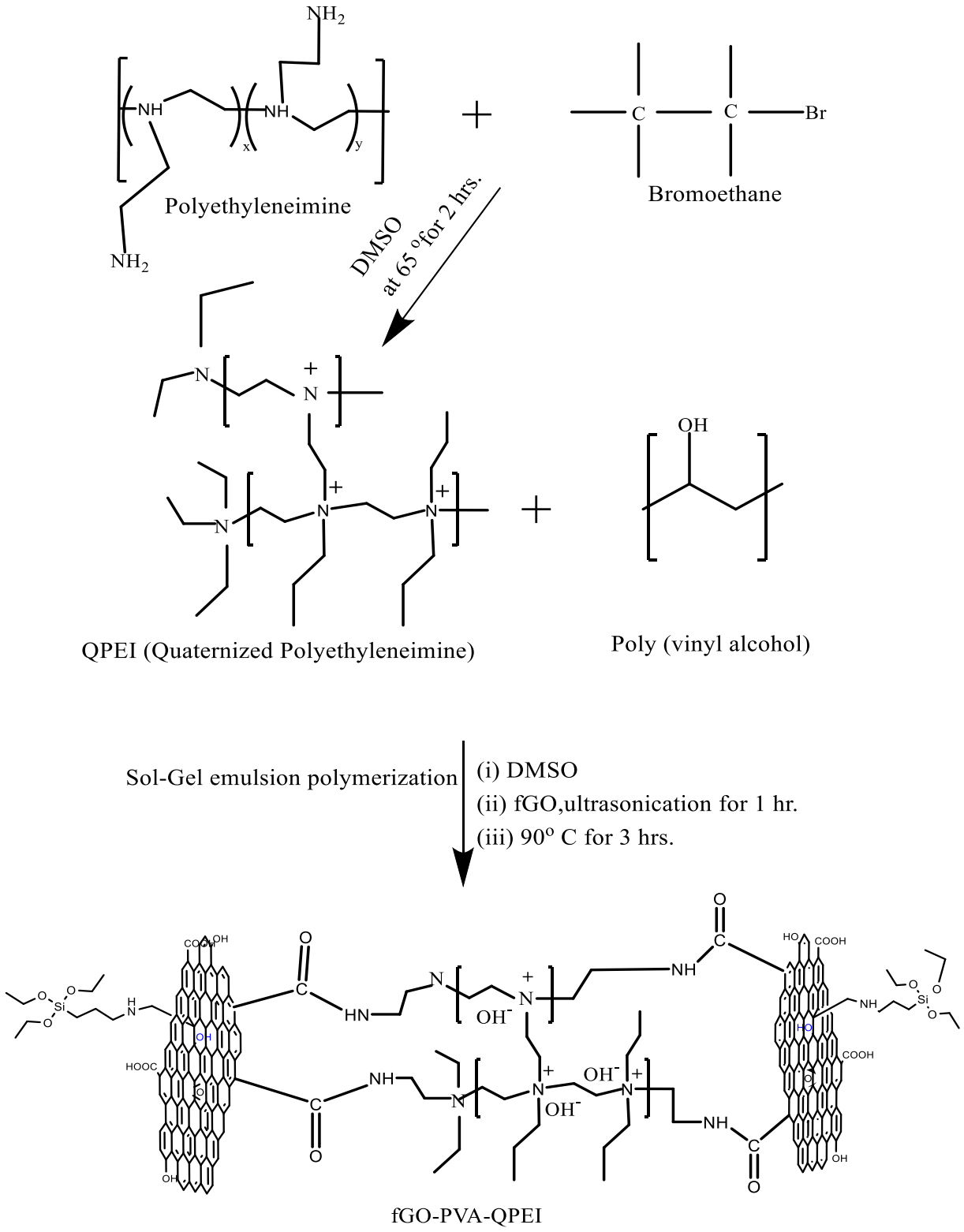

Scheme 2: Process for the preparation of *f* GO bases QPEI membrane

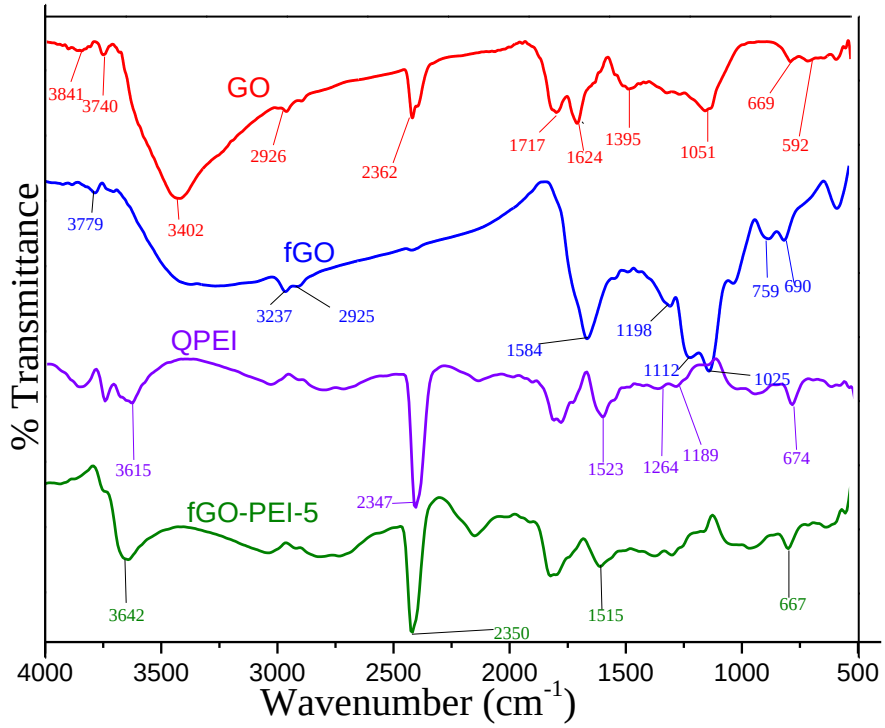

Fig. 1: FTIR spectrum of GO, *f* GO, Q PEI and *f* GO-PEI-5 membrane.

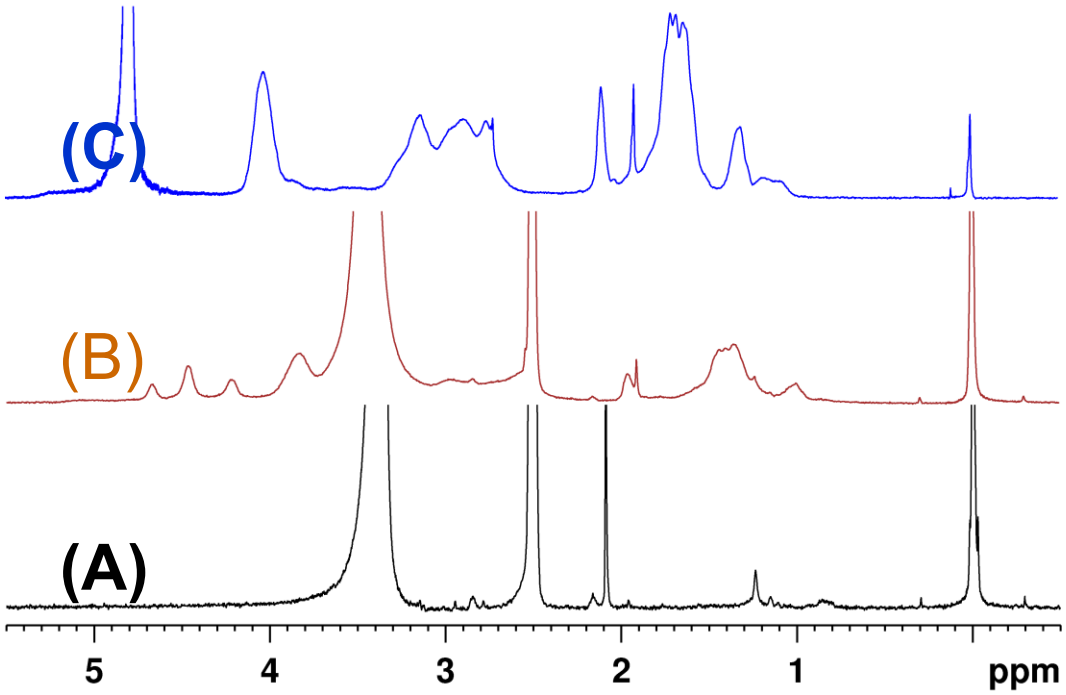

Fig. 2: NMR spectrum of (A) QPEI (B) *f* GO and (C) *f* GO-PEI

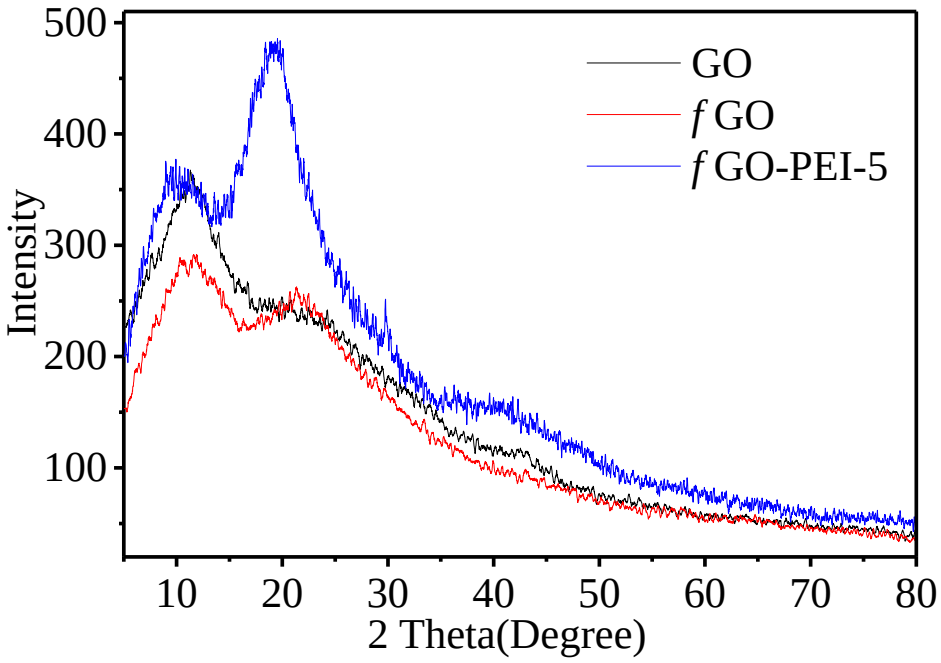

Fig. 3: XRD patterns for GO, *f* GO and *f* GO-PEI-5 membrane.

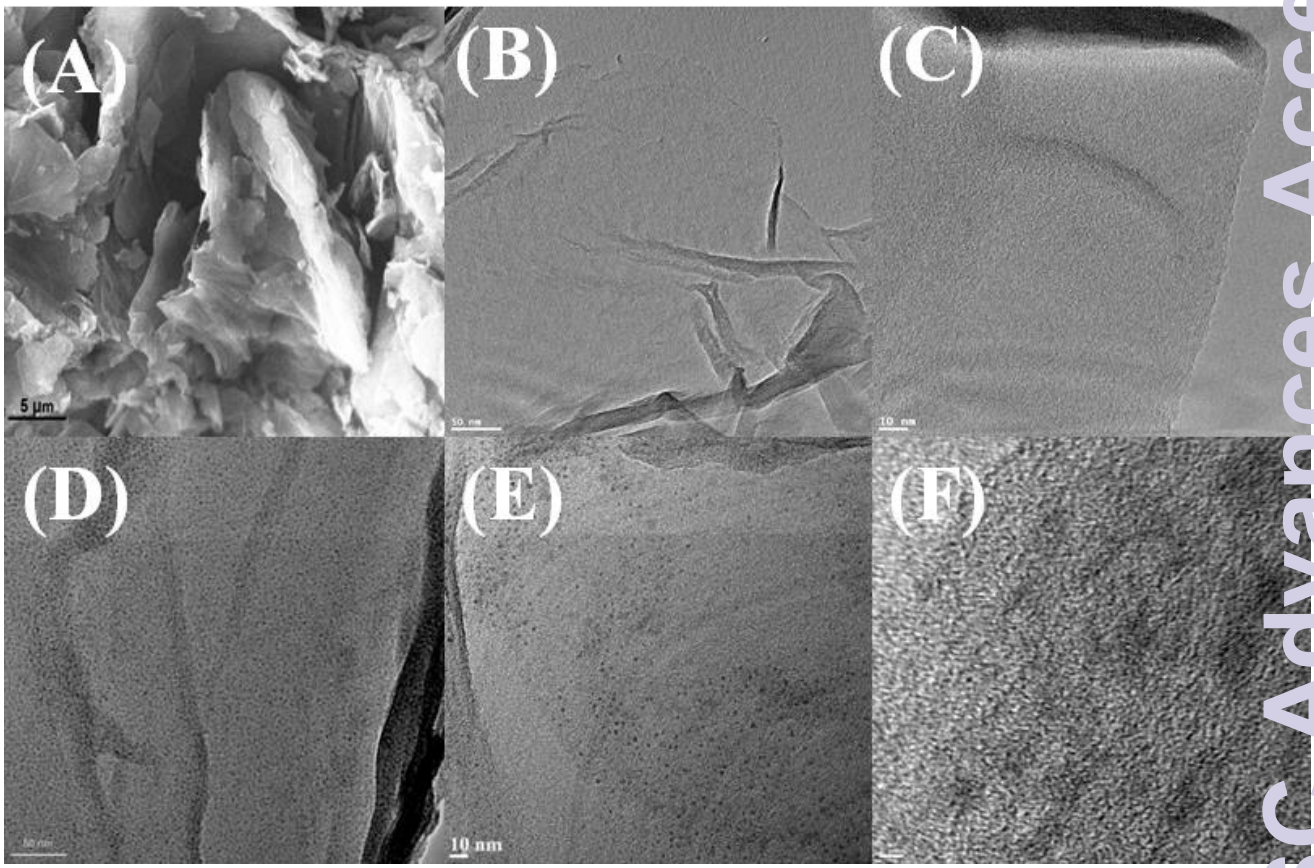

Fig. 4: SEM image of *f* GO (A) TEM images for GO (B, C) and *f* GO (D,E & F) at different magnification.

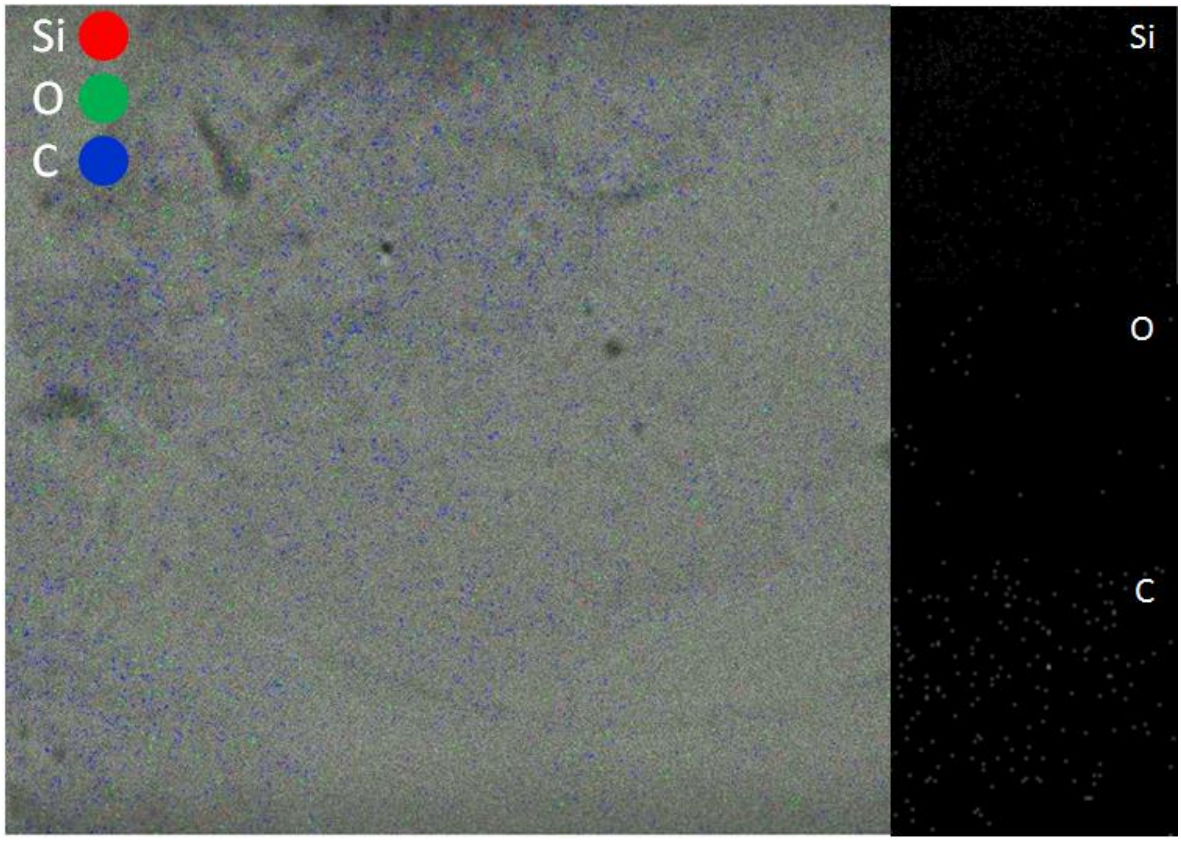

Fig. 5: Elemental mapping of *f* GO.

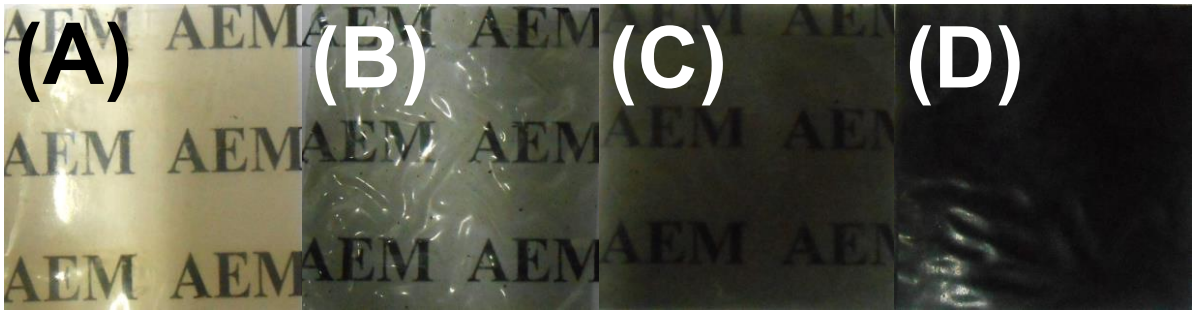

Fig. 6: Optical photograph of (A) QPEI (B) *f* GO-PEI-1 (C) *f* GO-PEI-2 and *f* GO-PEI-5 membranes.

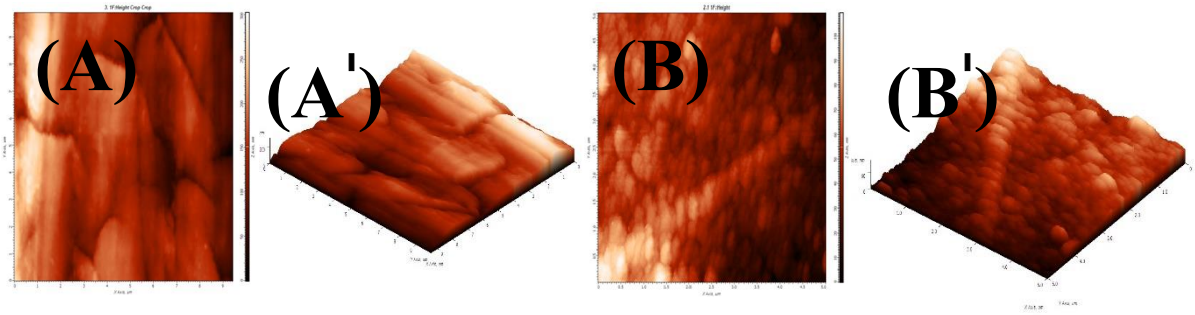

Fig. 7: AFM images of *f* GO-PEI-1 (A, A') and *f* GO-PEI-5 (B, B') membranes.

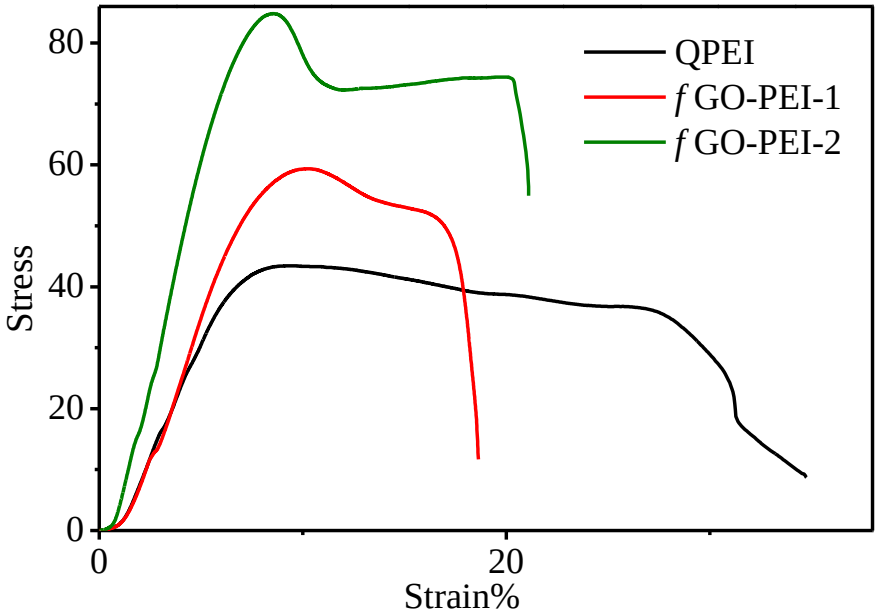

Fig. 8: Strain-Stress curves for QPEI & *f* GO-PEI membranes

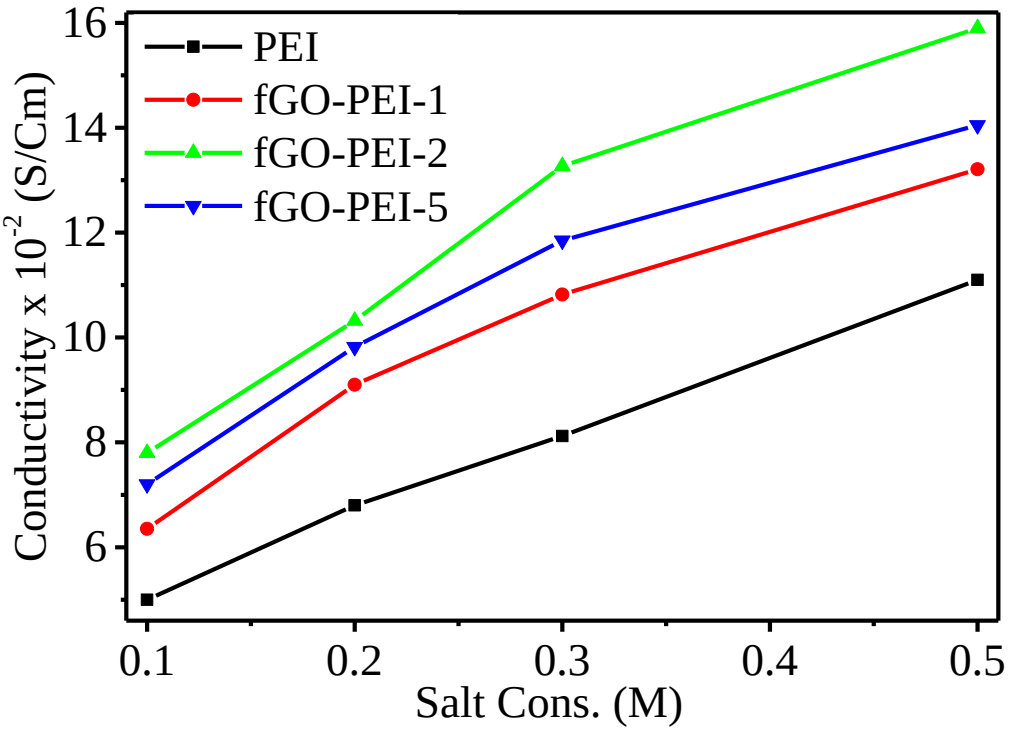

Fig. 9: Salt concentration versus ionic conductivity for different membranes

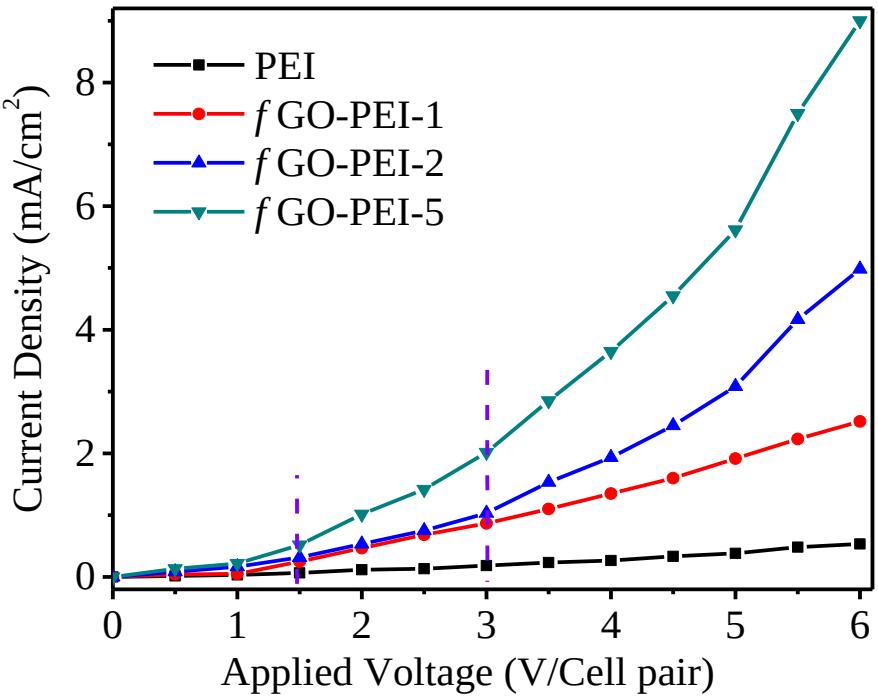

Fig. 10: Applied potential versus current density curves for different membranes

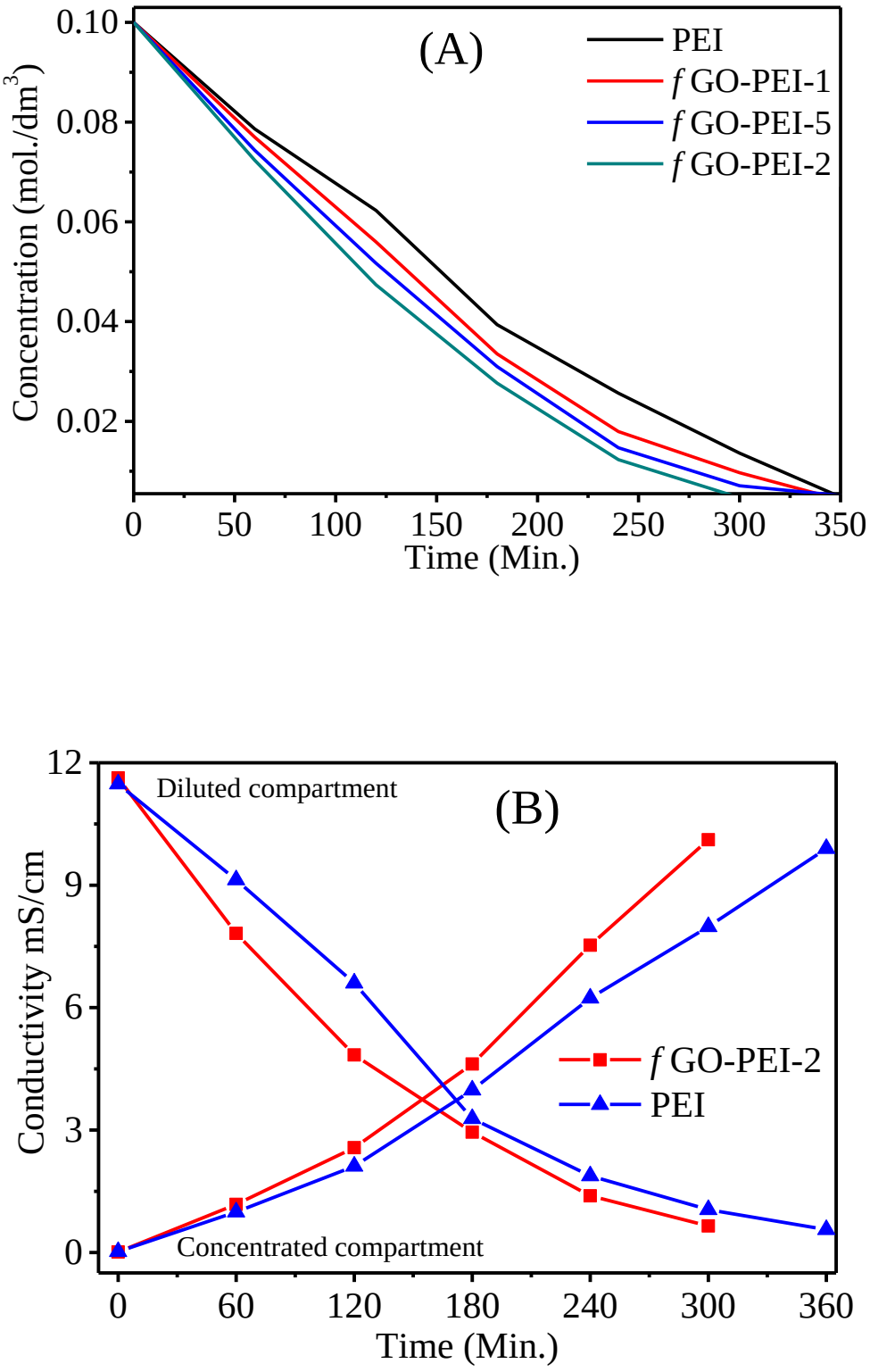

Fig. 11: Time versus (A) reduction in salt concentration and (B) reduction in conductivity in dil. compartment & increment in conductivity in cons. compartment, curves for different membranes

Table 1: Mechanical strength (Elastic modulus, Stress and Strain) for different membranes

Membrane Type	Elastic Modulus (MPa)	Stress (MPa)	Strain %
QPEI	12.6	43.43	34.6
f GO-PEI-1	6.47	59.26	18.6
f GO-PEI-2	6.31	84.78	21.1

Table 2: Ion exchange capacity (IEC), water uptake (%), counter ion transport number (t_m), bound and free water (%) and dimensional stability (%) for different membranes

Membrane Type	IEC (meq./g)	Transport number (t_m)	Water uptake %	Bound water %	Free Water %	Dimensional Change %
QPEI	2.65	0.81	40	0.6	39.4	45
f GO-PEI-1	2.85	0.82	43	0.8	42.2	42
f GO-PEI-2	3.31	0.89	57	1.2	55.8	38
f GO-PEI-5	2.83	0.87	61	1.3	59.7	33

Table 3: Membrane ionic conductivity (σ), Diffusion coefficient (D_σ), Methanol permeability (*Pm*) and selectivity (*S*) of different membranes.

Membrane Type	σ (x 10^{-2}) ($S.cm^{-1}$)	D_σ (x 10^{-10}) m^2S^{-1}	*Pm* (x 10^{-7}) cm^2S^{-1}	*S* (x 10^4)
QPEI	5.0	1.952	4.827	5.66
f GO-PEI-1	6.35	2.498	4.156	6.96
f GO-PEI-2	7.8	2.912	3.958	8.14
f GO-PEI-5	7.2	2.941	4.035	7.51

Table 4: Desalination performance (Efficiency and power consumption) of different membranes

Membrane Type	Current Efficiency η (%)	P/kW h kg^{-1} salt
QPEI	83.5	1.097
f GO-PEI-1	92.84	0.937
f GO-PEI-2	93	0.86
f GO-PEI-5	94.01	0.98